Fast Track Communications
IOP Publishing
Nanotechnology
Nanotechnology **25** (2014) 461001 (5pp)
doi:10.1088/0957-4484/25/46/461001

Fast Track Communication

Distinguishing ferritin from apoferritin using magnetic force microscopy

Tanya M Nocera[1], **Yuzhi Zeng**[1] **and Gunjan Agarwal**[1,2]

[1] Department of Biomedical Engineering, The Ohio State University, Columbus 43210, USA
[2] Davis Heart and Lung Research Institute, The Ohio State University, Columbus 43210, USA

E-mail: agarwal.60@osu.edu

Received 20 August 2014, revised 5 October 2014
Accepted for publication 13 October 2014
Published 30 October 2014

Abstract

Estimating the amount of iron-replete ferritin versus iron-deficient apoferritin proteins is important in biomedical and nanotechnology applications. This work introduces a simple and novel approach to quantify ferritin by using magnetic force microscopy (MFM). We demonstrate how high magnetic moment probes enhance the magnitude of MFM signal, thus enabling accurate quantitative estimation of ferritin content in ferritin/apoferritin mixtures *in vitro*. We envisage MFM could be adapted to accurately determine ferritin content in protein mixtures or in small aliquots of clinical samples.

Keywords: ferritin, iron-storage, magnetic force microscopy, apoferritin

(Some figures may appear in colour only in the online journal)

1. Introduction

Ferritin is an iron storage protein with a shell diameter, $d \sim 12$ nm [1]. It binds $\leqslant$4500 iron atoms as superparamagnetic ferrihydrite [2, 3]. Because of its correlation to total body iron content, ferritin levels are commonly used to monitor iron-deficiency or overload in patients. However, in certain circumstances such as inflammation, infection or injury, ferritin levels are inequitable with elevated iron [4–7]. It is speculated that this inconsistency is due to up-regulation of the iron-deficient protein, apoferritin. Antibody-based tests like enzyme-linked immunosorbant assays (ELISAs) and immunohistochemistry measure total apo/ferritin protein content irrespective of iron ligation. Further, small traces of iron cannot be resolved with Perls' staining or biochemical assays. The ability to distinguish ferritin from apoferritin in biological samples may therefore help improve diagnostics and treatment of imbalanced iron homeostasis.

Aside from its clinical relevance, ferritin has also been widely used for nanoparticle synthesis and for labeling biomolecules. In particular, the apoferritin shell has been used to encapsulate different types of atoms or compounds with controlled core diameters. Some examples of this include the synthesis of ferrimagnetic magnetite [8], superconducting cadmium sulfide nanoparticles used for fluorescent labeling [9], and the creation of magnesium, cobalt and copper nanoparticles with magnetic or conductive properties for applications in electronics [10]. Iron-bound ferritin has also been used as an alternative to immuno-gold to localize biomolecules using transmission electron microscopy [11, 12]. Detection of iron bound ferritin thus holds widespread relevance for both *in vitro* and *in vivo* studies.

Here we demonstrate how magnetic force microscopy (MFM) can be employed to distinguish ferritin from apoferritin. MFM is an atomic force microscopy (AFM)-based technique in which a magnetic probe is scanned at 'lift' heights (z) above the sample and long-range magnetic probe-sample interactions are recorded [13]. MFM requires small sample volumes (<50 μl) and offers exceptionally high sensitivity and resolution. Previous studies by us [14, 15] and others [16, 17] have used MFM to characterize superparamagnetic nanoparticles and distinguish magnetic from non-magnetic nanoparticles. Ferritin and apoferritin have also been distinguished in air and in liquid using MFM probes and a custom-designed bimodal force microscopy technique [18]. Using this approach the magnetic and mechanical

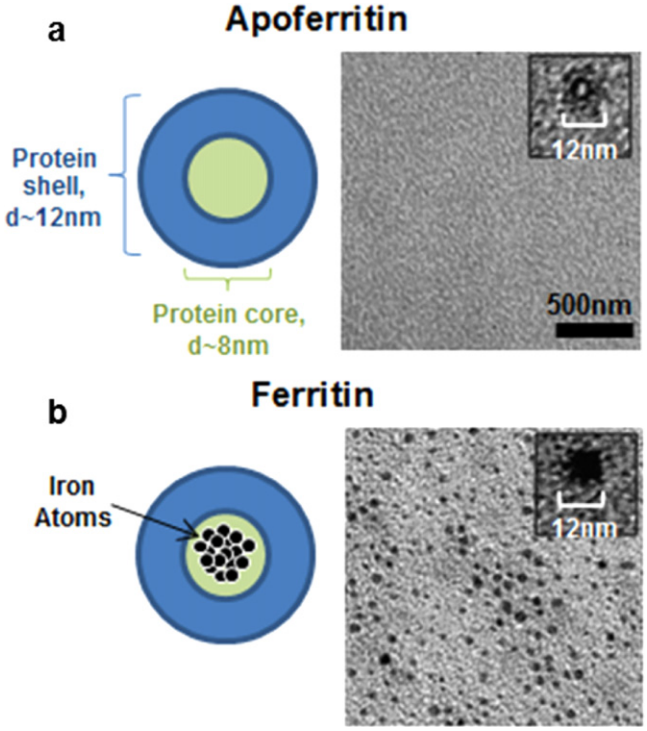

Figure 1. Transmission electron microscopy (TEM) of unstained (a) apoferritin and (b) ferritin samples show iron cores only in ferritin. Staining revealed protein shells (insets).

contributions to the phase shift could be separated. Although there has been evidence that MFM on commercial AFM instrumentation can detect ferritin *in vitro* [19], its ability to identify ferritin from apoferritin has not been adequately investigated. We demonstrate MFM as a novel approach to identify ferritin at the ultra-sensitive levels in ferritin/apoferritin mixtures *in vitro*.

2. Experimental

2.1. Transmission electron microscopy (TEM)

Purified apoferritin and ferritin proteins (Sigma-Aldrich, St. Louis, MO, USA) were from equine spleen. The proteins were diluted in milli-Q water to a final concentration of 1 μg ml^{-1}. Approximately 15 μl of each protein solution was aliquoted onto copper-coated TEM grids and allowed to sit at room temperature for 10 min. The grids were blotted and washed two times with milli-Q water and allowed to air-dry either overnight (unstained samples) or for one hour (stained samples). Approximately 5 μl of 1% uranyl acetate was placed on the stained samples for thirty seconds; the grids were then blotted and allowed to air-dry overnight. Grids were imaged with a Zeiss 900 TEM operated at 80 KeV (Carl-Zeiss SMT, Peabody, NY, USA). Digital micrographs were collected using an Olympus SIS Megaview III camera (Olympus, Lakewood, CO, USA). Core diameters and their standard deviations for ferritin ($n = 100$) proteins and shell diameters for apoferritin and ferritin proteins (both $n = 100$) were measured using ImageJ software (NIH, Bethesda, Maryland, USA).

2.2. Magnetic force microscopy (MFM)

Apoferritin and ferritin stock solutions were diluted in milli-Q water, and then mixed in five different ratios (0%, 25% 50%, 75% and 100% ferritin) with a total protein concentration of 1 μg ml^{-1}. To reduce aggregation, the protein solutions was vortex mixed briefly for 10–15 s prior to immobilization on substrates. Approximately 30 μl of each protein solution was aliquotted onto thin, freshly cleaved mica substrates (Ruby muscovite, S&J Trading, Glen Oaks, NY, USA) and allowed to air-dry in ambient conditions overnight.

MFM imaging was performed on a Multimode atomic force microscope (AFM) equipped with a Nanoscope IIIa controller and Quadrex extender (Digital Instruments, Santa Barbara, CA, USA). Samples were attached directly to the base of the JV scanner using a double-stick adhesive tape without the metallic stub commonly used to mount AFM samples. This enabled the samples to experience a magnetic field of 0.2 T emanating from the permanent magnet inherently present at the base of this scanner [14, 15] during imaging. MFM was performed using high magnetic moment probes (ASYMFM-HM, Asylum Research, Goleta, CA, USA) that were pre-magnetized with a permanent magnet for 2 min prior to use. All probes were auto-tuned to the manufacturer specified resonance frequency (70 kHz) with a 5% offset for main controls and 0% offset for interleave controls. Height and phase images were obtained in tapping mode at a scan rate of 2 Hz and at 512 lines/scan direction. The oscillation amplitude of the probe was between 0.7 nm and 3.7 nm. Height images were collected in the first pass, and phase images were collected in interleave lift mode at increasing lift heights ($z = 10$ to 50 nm). At least three independent experiments per sample type were conducted.

Images were flattened and the lateral width and phase shift for $n = 100$ particles per sample type were analyzed using the section analysis tool in the NanoScope Analysis software v. 1.40 (Bruker Corporation, Santa Barbara, CA, USA). Lateral widths were corrected based on the geometric deconvolution method ($d \approx 4\sqrt{Rr}$) as described earlier [15]. The deconvoluted lateral diameter (2r) was determined using the measured topographical diameter, d, and the average radius, R, of the MFM probe (~100 nm, manufacturer specified). Particles with a lateral width corresponding to the diameter of single apoferritin and ferritin proteins (13.2 ± 1.1 nm) were selected for phase shift analysis ($n = 50$) and are referred to as ~13 nm particles.

2.3. Protein and iron assays

Apoferritin and ferritin stock solutions were diluted in milli-Q water, and then mixed in five ratios (0%, 25% 50%, 75%, and 100% ferritin) with a total protein concentration of 300 μg ml^{-1}. Protein concentrations were confirmed using the Bio-Rad DC Protein Assay (Bio-Rad, Hercules, CA, USA) at a wavelength of 750 nm. For the iron assay, 50 μl of each

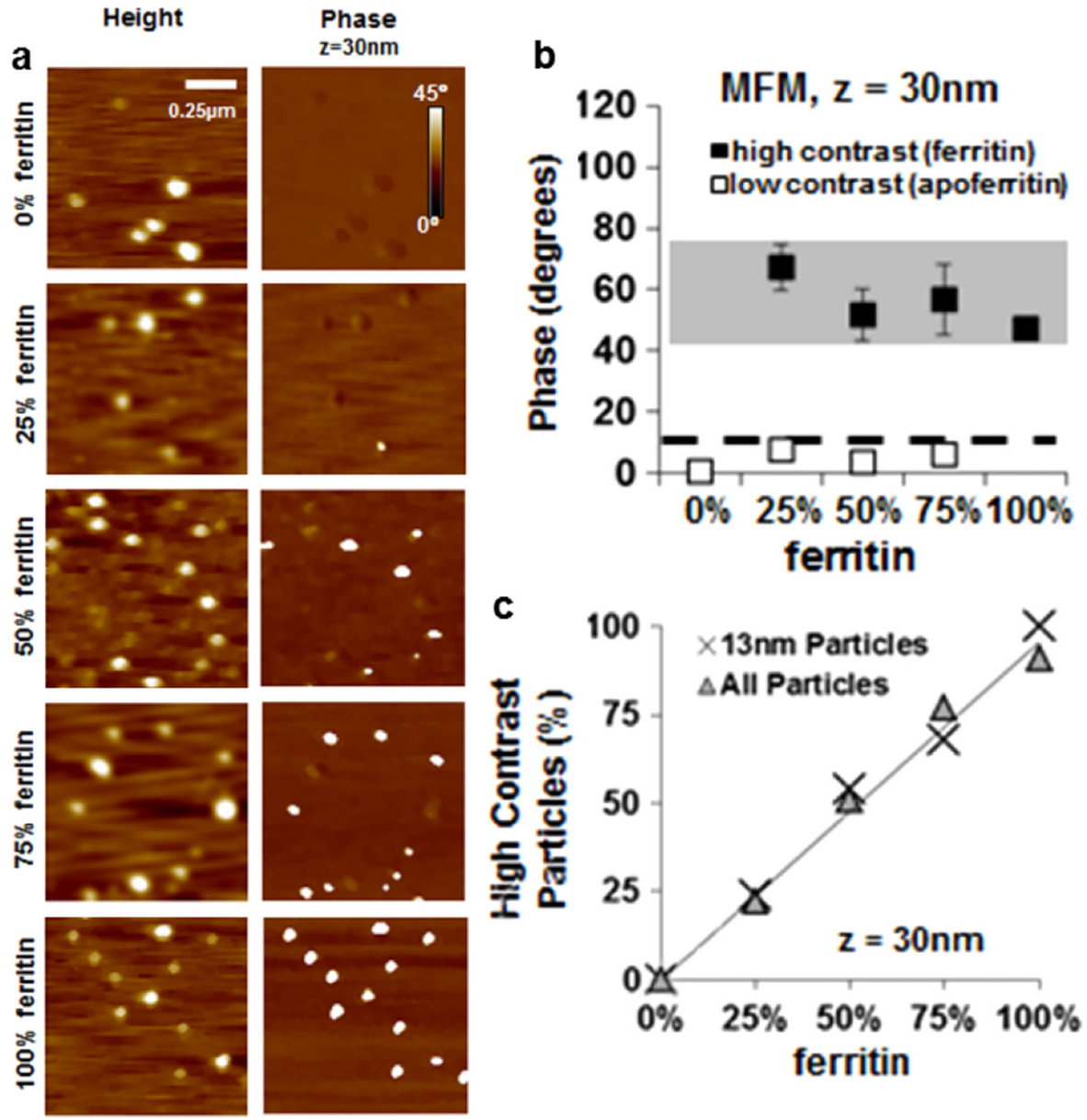

Figure 2. (a) MFM images of apoferritin/ferritin mixtures containing 1 μg ml^{-1} total protein. (b) MFM Phase contrast values for particles in various samples. Shaded areas represent phase ranges for ferritin using high moment probes; dotted lines represent approximate phase of ferritin reported using medium moment probes [19]. (c) Percentage of high contrast particles in MFM phase images matched predicted ferritin content ($R^2 = 0.99$) irrespective of particle size.

protein solution was mixed in a glass vial with 100 μl of 2 M H_2SO_4 and 100 μl of 0.5 mM dihydroxyfumaric acid (both from Sigma-Aldrich, St. Louis, MO, USA) and incubated at room temperature for 30 min to allow for the protein shells to be stripped. Next, 200 μl of 2.5 M NaOAc (Sigma-Aldrich, St. Louis, MO, USA) and 100 μl of 1 mM ferrozine (Fischer Scientific, Waltham, MA, USA) were mixed into the each vial and allowed to incubate at room temperature for another 30 min. Finally, each solution was diluted with 700 μl of milli-Q water. A 1 ml aliquot of each solution was then placed into a cuvette and measured with a DU730 Life Science UV/Vis spectrophotometer (Beckman-Coulter, Pasadena, CA, USA). Absorbance was recorded at a wavelength of 561 nm.

3. Results

Protein diameters and the presence of iron cores in ferritin were verified using TEM (figure 1).

To test whether MFM could quantify ferritin, samples with identical total protein concentration of 1 μg ml^{-1} (ferritin plus apoferritin) but varying ferritin content were analyzed (figure 2(a)). Pure apoferritin samples exhibited particles with low phase (<10°), whereas pure ferritin consistently exhibited higher phase (45.9 ± 5.6°) at a lift height (z) of 30 nm. As expected, MFM of apoferritin/ferritin mixtures revealed a mixture of particles with either low or high phase contrast (figure 2(b)). To quantify ferritin, we ascertained the

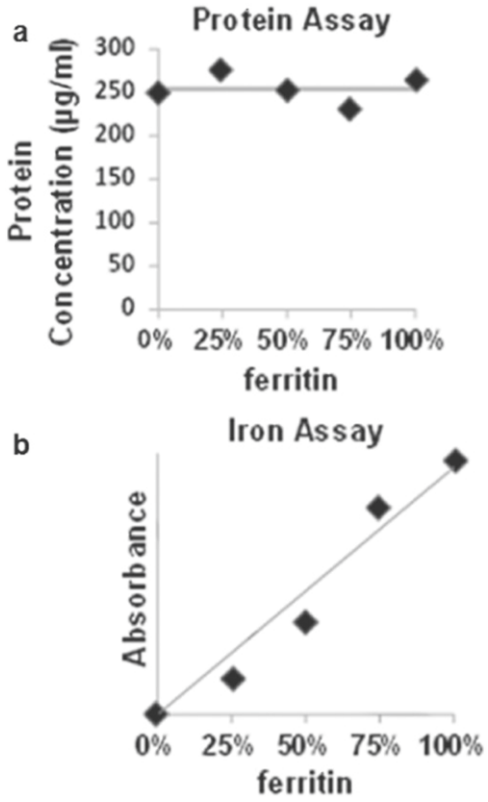

Figure 3. (a) Protein concentration and (b) iron absorbance are measured from 300 μg ml^{-1} total protein mixtures of apoferritin and ferritin.

percentage of high contrast particles in each sample (figure 2(c)). These percentages closely matched predicted ferritin content irrespective of particle size.

We compared MFM results to spectrophotometric measurements of protein (figure 3(a)) and iron (figure 3(b)) content in samples with total protein concentration of 300 µg ml^{-1} and increasing ferritin content. Protein concentrations, as expected, stayed the same while absorbance for iron concentration increased linearly with percentage of ferritin.

4. Discussion

Our ferritin phase contrasts obtained using high-moment (HM) probes are over three times greater in magnitude than those reported earlier using MFM with medium moment (MM) probes [19]. The increased sensitivity of the HM MFM probe, which is due to its higher probe moment, clearly contributes to the higher phase contrast of ferritin [14, 18]. In addition, other factors like particle orientation or saturation could contribute to the higher MFM signal. We as well as earlier studies [19] could not detect magnetic anisotropy of ferritin using MFM. However, studies using other techniques have elucidated that ferritin does possess magnetic anisotropy [20, 21]. It is possible that the HM MFM probe may impact the easy-axis orientation of the iron core in the ferritin cage and/or increase the induced magnetic moment in ferritin, either of which could also result in increased phase contrast. We thus demonstrate that the high moment MFM probes used in this study enabled us to enhance the phase differences between ferritin and apoferritin as compared to the earlier report [19]. Minor deviations in phase contrast for ferritin observed in our study may arise due to factors such as differences in size or chemical composition of iron core and/or variations in magnetic moments of MFM probes. We did not observe particle detachment from the surface even after repeated scanning with the HM MFM probes.

We additionally show how MFM can overcome limitations of biochemical assays such as ELISA, which fail to distinguish between ferritin and apoferritin levels. Also, unlike iron-chelation assays, MFM can quantitatively ascertain ferritin content at physiological concentrations in small sample volumes. MFM, together with existing clinical tests, may thus help elucidate ferritin from apoferritin in pathological samples. Further work employing quantitative estimates of MFM probe magnetic moment may also aid in ascertaining iron-core sizes and composition in ferritin samples.

5. Conclusions

We elucidate how MFM can detect ferritin based on the magnetic signature of iron cores. Major advantages of MFM for analyzing biological samples include its high sensitivity and spatial resolution and the ability to analyze samples with very low volume and ferritin concentrations, which are typically non-detectable using conventional biochemical assays. MFM may therefore serve as a novel and complementary analytical tool to improve our understanding of iron homeostasis. In addition, MFM could be useful to localize exogenously added ferritin labels in biological samples at the single-molecule and sub-cellular levels, which has thus far only been accomplished using electron microscopy.

Acknowledgments

We are grateful to Edward Calomeni of OSU College of Medicine for use of TEM. This work was supported by the Department of Biomedical Engineering, a facility grant from the Institute of Materials Research at The Ohio State University and in part by the NSF CBET award 1403574.

References

[1] Crichton R R 1973 Ferritin *Metal Bonding in Proteins* ed J D Dunitz, P Hemmerich, J A Ibers, C K Jorgensen, J B Neilands, D Reinen and R J P Williams (New York: Springer) pp 67–134
[2] Kilcoyne S H and Cywinski R 1995 Ferritin: a model superparamagnet *J. Magn. Magn. Mater.* **140–144** 1466–7
[3] Jambor J L and Dutrizac E 1998 Occurrence and consitution of natural and synthetic ferrihydrite, a widespread iron oxyhydroxide *Chem. Rev.* **98** 2549–86

[4] Patel S, Monemian S, Khalid A and Dosik H 2011 Iron deficiency anemia in adult onset Still's Disease with a serum ferritin of 26 387 μg L^{-1} *Anemia* **2014** 184748
[5] Smith R J, Davis P, Thomson A B, Wadsworth L D and Fackre P 1977 Serum ferritin levels in anemia of rheumatoid arthritis *J. Rheumat.* **4** 389–92
[6] Bari M A, Sutradhar S R, Sarker C N, Ahmed S, Miah A H, Alam M K, Hasan M J, Tariquzzaman M and Shamsi S 2013 Assessment of anaemia in patients with rheumatoid arthritis *Mymensingh Med. J.* **22** 248–54
[7] Fishbane S, Kalantar-Zadeh K and Nissenson A R 2004 Serum ferritin in chronic kidney disease: reconsidering the upper limit of iron treatment *Semin. Dial.* **17** 336–41
[8] Meldrum F, Heywood B and Mann S 1992 Magnetoferritin: *in vitro* synthesis of a novel magnetic protein *Science* **257** 522–3
[9] Iwahori K and Yamashita I 2008 Size-controlled one-pot synthesis of fluorescent cadmium sulfide semiconductor nanoparticles in an apoferritin cavity *Nanotechnology* **19** 495601
[10] Rakshit T and Mukhopadhyay R 2011 Tuning band gap of holoferritin by metal core reconsitution with Cu, Co, and Mn *Langmuir* **27** 9681–6
[11] Pringle G A and Dodd C M 1990 Immunoelectron microscopic localization of the core protein of decorin near the d and e bands of tendon collagen fibrils by use of monoclonal antibodies *J. Histochem. Cytochem.* **38** 1405–11
[12] Wang Q, Mercogliano C P and Löwe J 2011 A ferritin-based label for cellular electron cryotomography *Structure* **19** 147–54
[13] Agarwal G 2009 Characterization of magnetic nanomaterials using magnetic force microscopy *Magnetic Nanomaterials for Life Sciences* ed C Kumar (Weinhein, Germany: Wiley) pp 551–86
[14] Schreiber S, Savla M, Pelekhov D V, Iscru D F, Selcu C, Hammel P C and Agarwal G 2008 Magnetic force microscopy of superparamagnetic nanoparticles *Small* **4** 270–8
[15] Nocera T M, Chen J, Murray C B and Agarwal G 2012 Magnetic anisotropy considerations in magnetic force microscopy studies of single superparamagnetic nanoparticles *Nanotechnology* **23** 495704
[16] Neves C S, Quaresma P, Baptista P V, Carvalho P A, Araujo J P, Pereira E and Eaton P 2010 New insights into the use of magnetic force microscopy to discriminante between magnetic and nonmagnetic nanoparticles *Nanotechnology* **21** 305706
[17] Block S, Glöckl G, Weitschies W and Helm C A 2011 Direct visualization and identification of biofunctionalized nanoparticles using a magnetic atomic force microscope *Nano Lett.* **11** 3587–92
[18] Dietz C, Herruzo E T, Lozano J R and Garcia R 2011 Nanomechanical coupling enables detection and imaging of 5 nm superparamagnetic particles in liquid *Nanotechnology* **22** 125708
[19] Hsieh C W, Zheng B and Hsieh S 2010 Ferritin protein imaging and detection by magnetic force microscopy *Chem. Commun. (Camb.)* **46** 1655–165
[20] Allen P D, St Pierre T G, Chua-Anusorn W, Ström V and Rao K V 2000 Low-frequency low-field magnetic susceptibility of ferritin and hemosiderin *Biochim. Biophys. Acta—Mol. Basis Disease* **1500** 186–96
[21] Koralewski M, Pochylski M and Gierszewski J 2013 Magnetic properties of ferritin and akaganeite nanoparticles in aqueous suspension *J. Nanoparticle Res.* **15** 1902